Journal of Applied Fluid Mechanics, Vol. 9, No. 5, pp. 2267-2276, 2016.
Available online at www.jafmonline.net, ISSN 1735-3572, EISSN 1735-3645.
DOI: 10.18869/acadpub.jafm.68.236.25049

Wave Transformation Modeling with Effective Higher-Order Finite Elements

T. H. Jung[1] and Y. Ryu[2†]

[1] *Department of Civil and Environmental Engineering, Hanbat National University, 125 Dongseodaero, Yuseong-gu, Daejeon 305-719, Republic of Korea*
[2] *Hydro Science and Engineering Research Institute, Korea Institute of Civil Engineering and Building Technology, 283 Goyangdaero, Ilsanseo-gu, Goyang, Gyeonggi-do 411-712, Republic of Korea*

†*Corresponding Author Email: yuryu@kict.re.kr*

(Received May 8, 2015; accepted October 14, 2015)

ABSTRACT

This study introduces a finite element method using a higher-order interpolation function for effective simulations of wave transformation. Finite element methods with a higher-order interpolation function usually employ a Lagrangian interpolation function that gives accurate solutions with a lesser number of elements compared to lower order interpolation function. At the same time, it takes a lot of time to get a solution because the size of the local matrix increases resulting in the increase of band width of a global matrix as the order of the interpolation function increases. Mass lumping can reduce computation time by making the local matrix a diagonal form. However, the efficiency is not satisfactory because it requires more elements to get results. In this study, the Legendre cardinal interpolation function, a modified Lagrangian interpolation function, is used for efficient calculation. Diagonal matrix generation by applying direct numerical integration to the Legendre cardinal interpolation function like conducting mass lumping can reduce calculation time with favorable accuracy. Numerical simulations of regular, irregular and solitary waves using the Boussinesq equations through applying the interpolation approaches are carried out to compare the higher-order finite element models on wave transformation and examine the efficiency of calculation.

Keywords: Finite element method; Boussinesq equations; Lagrangian interpolation function; Legendre cardinal interpolation function.

1. INTRODUCTION

Waves approaching a beach transform in diverse ways through diffraction, refraction, and shoaling. The usual approach to simulating wave transformation and investigating its effects is to perform physical model experiments and numerical modeling. Rather than experiments, numerical simulations are performed for various coastal processes as they are less affected by economic and physical restrictions. Of the many numerical methods, a finite element method (FEM) has a complicated formulation process due to approximated solutions, but is very efficient for complex boundary features. With the merit, FEM has been frequently used for complex topography and coastal regions (Adytia and Groesen 2012; Panchang *et al*. 2000; Park *et al*. 1994; Patera 1984; Walkley and Berzins 2002; Wei and Jia 2014a, 2014b; Woo and Liu 2004b).

In FEM, a Lagrangian polynomial is mainly used to interpolate elements. When the governing equation is higher order differential equation such as Boussinesq-types equations, a higher-order element can be applied to a governing equation directly. However, a higher-order Lagrangian polynomial is used as an interpolation function, original equations become too complicated. For the reason, in most cases governing equations are formalized using a linear interpolation equation (Kato *et al*. 1998; Woo and Liu 2004a). Although the process to formalize governing equations with a linear interpolation function is simple, a large number of elements is needed to improve the accuracy of solutions. If there are many differential terms in governing equations, a linear interpolation function is limited in application. In this case, the use of higher-order elements is unavoidable (Sanz-Serna and Christie 1981; Woo and Liu 2001). If a higher-order Lagrangian (or Hermite type) polynomial is used, nodes within elements should be mostly distributed at equal intervals. In this approach, some problems may arise. First, a great deal of time is required to acquire a solution since the degree of a polynomial increases. Secondly, although mass lumping, which is a way to make a full matrix into a diagonal matrix, is performed to reduce calculation time, this method lowers the accuracy of solutions. Note that mass lumping makes a diagonal matrix through

summing up all elements in a row of a mass matrix to leave one element with the rest of 0 in a corresponding row. The problem of solution accuracy being reduced due to mass lumping can be offset by adjusting node locations within elements. Since the interpolation process through the node adjustment can be done using a Legendre polynomial, the interpolation function will be called the Legendre interpolation function hereinafter. The application of the Legendre interpolation function transforms a mass matrix into a diagonal matrix through numerical integration. Using the Legendre interpolation function, the numerical integration of a mass matrix leads to fast calculation with favorable accuracy, similar to conducting mass lumping. The method with the Legendre interpolation function is proposed by Patera (1984) and has been applied to simulations of gravity waves by Eskilsson and Sherwin (2003) and by Eskilsson *et al*. (2006). Note that while the method is noted as a spectral element method in their papers, the terminology is not used in this study because the application of higher-order polynomials explains the method more clearly. In both papers, the features of the Legendre interpolation function, an important point of the method, are not well explained. In Eskilsson and Sherwin (2003), the numerical integration of the high order Legendre interpolation function is compared with FEM modeling using a linear interpolation function to show its efficient calculation. Nonetheless, the comparison of the higher order Legendre interpolation function with the linear Lagrangian interpolation function lacks an explanation of the relative features of the methods because of the different linearity. In this study, in order to investigate the merits of the Legendre interpolation function in applications to wave transformation, the method is compared with the application of the Lagrangian interpolation function of the same degree. The comparisons are performed through calculations of the Boussinesq equations, which can consider weak non-linearity and dispersion (Nwogu 1993) with the methods.

2. THEORETICAL BACKGROUND

Ocean waves show various characteristics depending on relative water depth. In the deep water condition, the wave dispersion (σ: ratio of water depth to wave length) is significant. As a wave approaches the shallow water depth, wave dispersion becomes smaller, while non-linearity (ε: ratio of wave height to water depth) becomes bigger. Therefore, for simulations of wave characteristics, there is a need to use relevant governing equations that can consider both dispersion and non-linearity. The Boussinesq equations have been widely used for wave simulation. Since Peregrine (1967) proposed the former type of the equations for a model applicable to varying depth, the Boussinesq-type equations have been developed by many researchers such as Adytia and van Grosen (2012), Gobbi and Kirby (1999), Kim *et al*. (2009), Madsen *et al*. (1991), Nwogu (1993), Roeber *et al*. (2010), and Witting (1984).

2.1 Governing Equations

This study uses the Boussinesq equations presented in Eqs. (1) and (2), which were introduced by Nwogu (1993) for wave simulation. The Boussinesq equations model can simulate weakly non-linear ($\varepsilon \ll 1$) and weakly dispersive ($\sigma \ll 1$) waves.

$$\frac{\partial \eta}{\partial t} + \frac{\partial}{\partial x}\left((\eta + h)u\right) + \frac{\partial}{\partial x}\left(A_1 h^3 \frac{\partial^2 \eta}{\partial x^2} + A_2 h^2 \frac{\partial^2}{\partial x^2}(hu) \right) = 0 \tag{1}$$

$$\frac{\partial \eta}{\partial t} + \frac{\partial}{\partial x}\left(\frac{u^2}{2} + g\eta \right) + B_1 h^2 \frac{\partial^3 u}{\partial x^2 \partial t} + B_2 h \frac{\partial^2}{\partial x^2}\left(h \frac{\partial u}{\partial t} \right) = 0 \tag{2}$$

In the equations, η is the free water surface elevation, u is the horizontal velocity, h is the water depth, and A_1, A_2, B_1, and B_2 are the constants defined as follows:

$$A_1 = \frac{1}{2}\theta^2 - \frac{1}{6} \tag{3}$$

$$A_2 = \theta + \frac{1}{2} \tag{4}$$

$$B_1 = \frac{1}{2}\theta^2 \tag{5}$$

$$B_2 = \theta \tag{6}$$

where θ is the constant defined in Eq. (7).

$$\theta = \frac{z}{h} \tag{7}$$

In Eq. (7), z is the vertical distance measured from still water level. Nowgu (1993) compared the normalized phase and group velocities for different α and found that $\theta = -0.531$ yielded the smallest error; hence, the value of θ is usually used in the equations.

2.2 Formulation

Due to the higher-order differential term included in Eq. (1), two main methods are used to apply FEM to the Boussinesq equations. One of the methods is to use a higher-order interpolation function, whereas the other is to lower the higher-order differential term's order using auxiliary variables. This study formulated the equations using the latter method, proposed by Walkey and Berzins (1999). Eqs. (1) and (2) can be expressed as follows when the auxiliary variables are used:

$$\frac{\partial \eta}{\partial t} + \frac{\partial}{\partial x}\left((\eta + h)u\right) + \frac{\partial w}{\partial x} = 0 \tag{8}$$

$$\frac{\partial u}{\partial t}+\frac{\partial}{\partial x}\left(\frac{u^2}{2}+g\eta\right) + B_1h^2\frac{\partial^3 u}{\partial x^2\partial t}+B_2h\frac{\partial^2}{\partial x^2}\left(h\frac{\partial u}{\partial t}\right)=0 \tag{9}$$

$$w-A_1h^3\frac{\partial^2 u}{\partial x^2}-A_2h^2\frac{\partial^2}{\partial x^2}(hu)=0 \tag{10}$$

Applying the Galerkin method to Eqs. (8) ~ (10) with the assumption of constant water depth gives the following equations (Zienkiewicz and Taylor, 1989):

$$\mathbf{M}^e\frac{\partial \eta^e}{\partial t}=-\mathbf{D}^e\left(\left(h+\eta^e\right)u^e+w^e\right) \tag{11}$$

$$\left(\mathbf{M}^e-\left(b_1+b_2\right)h^2\mathbf{K}^e\right)\frac{\partial \eta^e}{\partial t} =-\mathbf{D}^e\left(\frac{\left(u^e\right)^2}{2}+g\eta^e\right) \tag{12}$$

$$\mathbf{M}^e w^e=-\left(a_1+a_2\right)h^3\mathbf{K}^e u^e \tag{13}$$

where η^e, u^e, and w^e are the values of η, u, and w at each node, respectively, and g is the gravitational acceleration. $\mathbf{M}^e$, $\mathbf{D}^e$, and $\mathbf{K}^e$ are the matrices defined as follows:

$$\mathbf{M}^e=\int_{-1}^{1}J^e\mathbf{N}\mathbf{N}^{\mathrm{T}}d\xi \tag{14}$$

$$\mathbf{D}^e=\int_{-1}^{1}\mathbf{N}\frac{\partial \mathbf{N}^{\mathrm{T}}}{\partial \xi}d\xi \tag{15}$$

$$\mathbf{K}^e=\int_{-1}^{1}\frac{1}{J^e}\frac{\partial \mathbf{N}}{\partial \xi}\frac{\partial \mathbf{N}^{\mathrm{T}}}{\partial \xi}d\xi \tag{16}$$

where J^e is the Jacobian, and $\mathbf{N}$ (or $[N_0\ N_1\ \cdots\ N_p]$) is the interpolation function of the $\boldsymbol{p}$ degree. For the interpolation function, the Lagrangian interpolation function expressed as Eq. (17) is used and the nodes are located with the same interval within the elements.

$$N_p(\xi)=\begin{cases}1, & \xi=\xi_p\\ \dfrac{\Pi_{q=0,q\neq p}^{p}\left(\xi-\xi_q\right)}{\Pi_{q=0,q\neq p}^{p}\left(\xi_p-\xi_q\right)}, & \text{otherwise}\end{cases},\ 0\le p\le P \tag{17}$$

In Eq. (17), L_p indicates the Legendre polynomial with the p degree and ξ_p is the location of the nodes within the elements. For the case of the Lagrangian interpolation function, these locations are distributed evenly with an element. In this case, as the terms of the interpolation function become a higher order, solving the matrix takes a long time. As a way to resolve the problem of the time increment, lumping can be applied to the mass matrix to make a diagonal matrix. However, mass lumping decreases the accuracy of the solutions (Walkley and Berzins 1999). As an alternative method to satisfy the needs of both calculation time and accuracy, the Legendre interpolation function proposed by Patera (1984) can be used for the calculation. This method can reduce the calculation time similarly to the effect by the mass lumping without lowering the solutions' accuracy. The interpolation function using the Legendre function can be formulated as follows:

$$N_p(\xi)=\begin{cases}1, & \xi=\xi_p\\ \dfrac{(\xi-1)(\xi+1)L_p'(\xi)}{P(P+1)L_p(\xi_p)(\xi_p-\xi)}, & \text{otherwise}\end{cases},\ 0\le p\le P \tag{18}$$

where L_p indicates the Legendre polynomial with the p degree and ξ_p is the location of the nodes within the elements satisfying $(\xi-1)(\xi+1)\partial_\xi L_p(\xi)=0$. When a cubic polynomial is used, Eqs. (17) and (18) are formulated in the following equations showing the distributions in Fig. 1.

For the Lagrangian interpolation function:

$$N_1=\frac{1}{16}(1-\xi)(-1+3\xi)(1+3\xi) \tag{19a}$$

$$N_2=\frac{9}{16}(-1+\xi)(1+\xi)(-1+3\xi) \tag{19b}$$

$$N_3=-\frac{9}{16}(-1+\xi)(1+\xi)(1+3\xi) \tag{19c}$$

$$N_4=\frac{1}{16}(1+\xi)(-1+3\xi)(1+3\xi) \tag{19d}$$

For the Legendre interpolation function:

$$N_1=\frac{(\xi-1)\left(\sqrt{5}\xi+1\right)\left(\sqrt{5}\xi-1\right)}{-8} \tag{20a}$$

$$N_2=\frac{5(\xi-1)(\xi+1)\left(\sqrt{5}\xi-1\right)}{8} \tag{20b}$$

$$N_3=\frac{5(\xi-1)(\xi+1)\left(\sqrt{5}\xi+1\right)}{-8} \tag{20c}$$

$$N_4=\frac{(\xi+1)\left(\sqrt{5}\xi+1\right)\left(\sqrt{5}\xi-1\right)}{8} \tag{20d}$$

Directly integrating Eqs. (14) ~ (16) generates a 4×4 matrix. By summing up those for all elements, a matrix with a bandwidth size of 4 is generated. In this case, as the number of elements increases, more calculation time is needed. Although the calculation time can be reduced by making a diagonal matrix using mass lumping, the accuracy of solutions decreases. If the Legendre matrix is used, the mass matrix can be transformed to a diagonal matrix by

carrying out the Gauss-Radau-Legendre numerical integration without mass lumping (Karniadakis and Sherwin 2005).

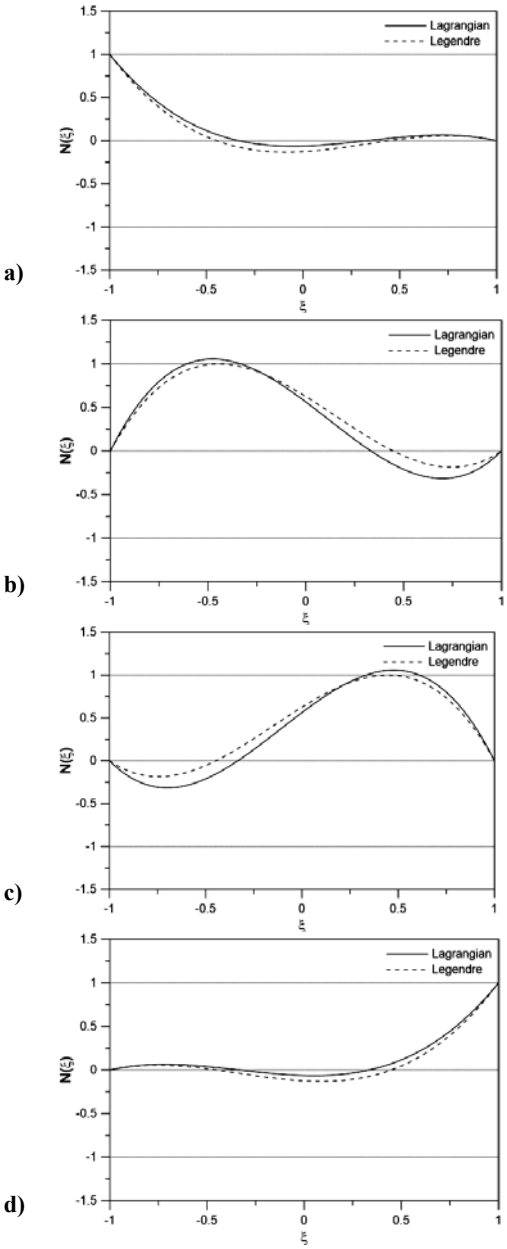

Fig. 1. Lagrangian and Legendre interpolation functions for third-order: a) N_1; b) N_2; c) N_3; d) N_4.

The basic concept of the Gauss-Radau-Legendre numerical integration is the same as a general Gauss integration. In other words, the integrated value of a function can be the sum of weight-multiplied function values of certain locations between -1 and 1. The difference from a general Gauss integration is that the location values of the Gauss-Radau-Legendre integration are the same as the node locations of the Legendre interpolation function. Consequently, the number of integration points is one more than that of degrees. The certain locations and weights are defined as follows:

$$\xi_i = \begin{cases} -1, & i = 0, \\ \xi^{1,1}_{i-1,P-1}, & i = 1, \cdots, P-1, \\ 1, & i = P \end{cases} \tag{21}$$

$$\alpha^{0,0}_1 = \frac{2}{P(P+1)\left[L_p(\xi_i)\right]^2}, \quad i = 0, \cdots, P \tag{22}$$

where $\alpha^{0,0}_i$ is a weighting factor for numerical integration. If calculating Eqs. (21) and (22) for the case of cubic higher-order elements, the values of the integration points are -1, $-1/\sqrt{5}$ $1/\sqrt{5}$, 1 and corresponding weights are 1/6, 5/6, 5/6, 1, respectively (see Karniadakis and Sherwin (2005) for details).

The differential values necessary for calculating Eqs. (15) and (16) are obtained as follows.

$$d_{ij} = \begin{cases} \dfrac{-P(P+1)}{4}, & i = j = 0 \\ \dfrac{L_P(\xi_i)}{L_P(\xi_j)} \dfrac{1}{\xi_i - \xi_j}, & i \neq j, 0 \le i, j \le P, \\ 0, & i = j, 1 \le i \le P-1, \\ \dfrac{P(P+1)}{4}, & i = j = P \end{cases} \tag{23}$$

Summing up the obtained matrices for each element gives the values of **M**, **D**, and **K**. With the values, η and u can be solved as follows:

$$\eta^{n+1} = \eta^n + \mathbf{M}^{-1} \frac{\Delta t}{12}\left(23\mathbf{E}^n - 16\mathbf{E}^{n-1} + 5\mathbf{E}^{n-2}\right) \tag{24}$$

$$u^{n+1} = u^n + \left[\mathbf{M} - \left(b_1 + b_2\right) h^2 \mathbf{K}\right]^{-1} \cdot \frac{\Delta t}{12}\left(23\mathbf{F}^n - 16\mathbf{F}^{n-1} + 5\mathbf{F}^{n-2}\right) \tag{25}$$

where n indicates the n^{th} time term, Δt is the time interval, and **E** and **F** denote the right hand-side term of Eqs. (11) and (12), respectively. With u^{n+1} which is solved from the above process, w^{n+1} can be obtained in the following equation.

$$w^{n+1} = -(a_1 + a_2) h^3 \mathbf{M}^{-1} \mathbf{K} u^{n+1} \tag{26}$$

3. SIMULATION RESULTS

This study investigates the applicability of a finite element model using the Legendre elements for regular, irregular and solitary wave conditions. For each type of the tested waves, different methods to solve the matrix equation, Eq. (14), were examined, as follows: full matrix calculation using the Lagrangian elements (La-A); diagonal matrix calculation through the mass lumping using the Lagrangian elements (La-B); full matrix calculation using the Legendre elements (Le-A); numerical

integration using the Legendre elements (Le-B). The solutions obtained by the approaches were compared to show the relative merits of each method using the Legendre functions.

In the case of the regular wave, the initial conditions and boundary conditions of the monochromatic wave were set as follows:

$$\eta(x,0) = \eta_0 \sin(kx) \tag{27a}$$

$$u(x,0) = c\eta(x,0) \tag{27b}$$

$$w(x,0) = -(a_1 + a_2) h^3 k^2 c\eta(x,0) \tag{27c}$$

$$\eta(x_1,t) = \eta_0 \sin(kx_1 - \omega t) \tag{27d}$$

$$u(x_1,t) = c\eta(x_1,t) \tag{27e}$$

$$w(x_1,t) = -(a_1 + a_2) h^3 k^2 c\eta(x_1,t) \tag{27f}$$

$$\eta(x_2,t) = \eta_0 \sin(kx_2 - \omega t) \tag{27g}$$

$$u(x_2,t) = c\eta(x_2,t) \tag{27h}$$

$$w(x_2,t) = -(a_1 + a_2) h^3 k^2 c\eta(x_2,t) \tag{27i}$$

where x_1 and x_2 are the spatial starting and ending points of the domain area, η_0 is the amplitude, and k is the wavenumber. The wave velocity c and the angular velocity ω can be obtained, respectively, from the following equations:

$$c = \frac{\omega}{kh\left[1 - (a_1 + a_2) k^2 h^2\right]} \tag{28}$$

$$\frac{\omega^2}{ghk^2} = \frac{1 - (a_1 + a_2) k^2 h^2}{1 - (b_1 + b_2) k^2 h^2} \tag{29}$$

The numerical simulation of the regular waves was carried out under shallow water conditions. The relative water depth, kh, was 0.167 and the wave height of 0.01 m and the water depth of 3.2 m were set to meet the weak nonlinearity. The time interval, Δt, was 0.01 sec to minimize any numerical error related to the time difference. Fig. 2 shows the results of the calculation of the finite element model and the analytical solutions at $t = 0.5T$ and $t = 5T$.

Note that T indicates the incident wave period. In the computation, the grid per wavelength was divided into 10 and the Lagrangian and Legendre functions were used for an interpolation function. As shown in the figure, the numerical solutions are in good agreement with the analytical solutions.

To compare the accuracy of the solutions, the L^∞ error defined below was calculated and compared:

$$\left\| \eta - \bar{\eta} \right\|_{L^\infty} = \frac{\max_j \left| \eta_j - \bar{\eta}_j \right|}{\eta_0} \quad \text{for} \quad j = 1, \cdots, N_{dof} \tag{30}$$

where N_{dof} is the total number of nodes. Fig. 3 compares the errors between the numerical results and the analytical solutions depending on the number of elements for 10 wave periods. When the full matrix was solved directly, there was no big difference in the error between the FEM with the Lagrangian interpolation function (La-A) and that with the Legendre function (Le-A) as shown in Fig. 3a). The full matrix solutions start to converge, showing an error of O (10^{-1}) from the use of 3 elements per wave length. On the other hand, in the cases of the diagonal matrix, the FEM with the Lagrangian interpolation function (La-B) shows a difference from that with the Legendre function (Le-B). Overall, the method with the Legendre interpolation function shows smaller errors. On average, the error of Le-A is almost double that of Le-B, and the maximum error is almost seven times when the number of elements is two. For the method with the Lagrangian interpolation function, the error converges to O (10^{-1}) when 6 or more elements were used per wave length. Meanwhile, the error of the FEM with the Legendre interpolation function reaches O (10^{-1}) from 4 elements per wave length.

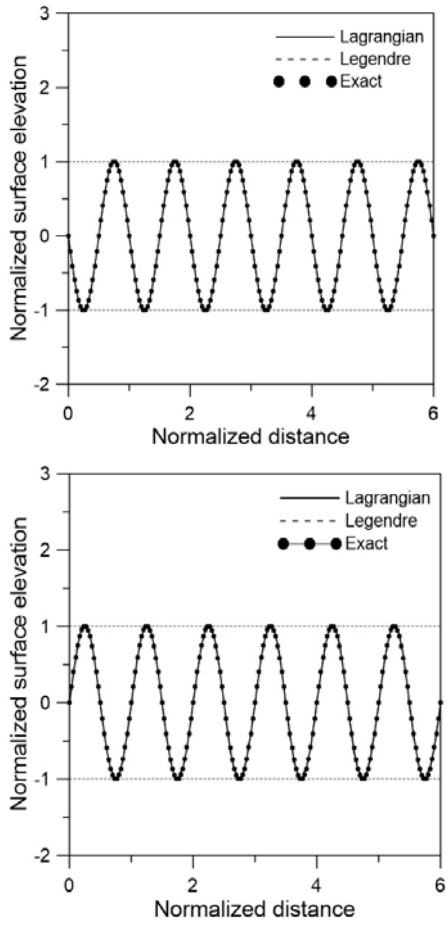

Fig. 2. Comparison of the regular wave solutions with the analytical solution for: a) $t = 0.5T$; b) $t = 5T$.

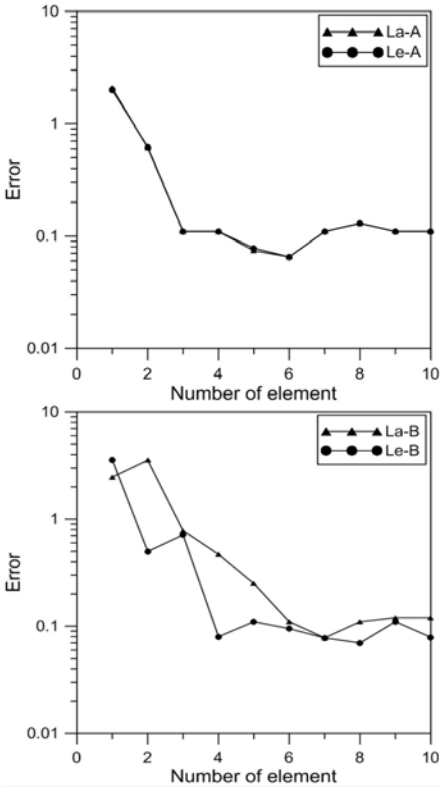

Fig. 3. Errors estimated by the Lagrangian (La) and Legendre (Le) interpolation functions for the regular waves: a) full matrix; b) diagonal matrix.

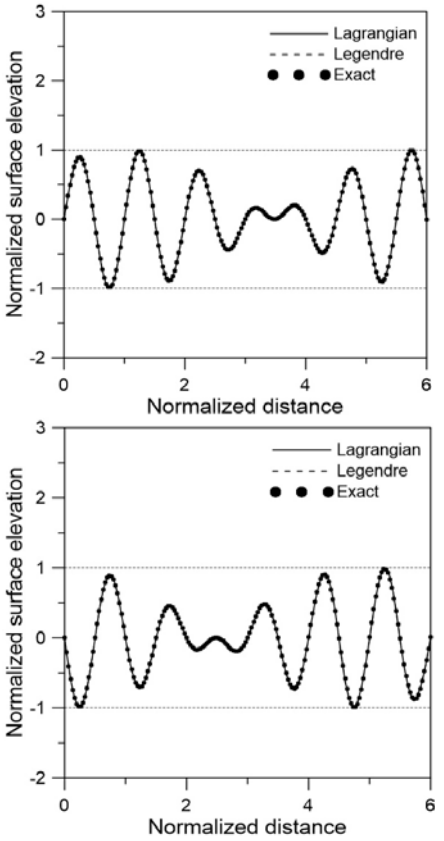

Fig. 4. Comparison of the irregular waves solutions with the analytical solution for: a) t = 1T; b) t = 5T.

Irregular waves are also considered to check the accuracy of the method. Irregular waves could be assumed as a sum of linear waves which have different heights, periods and phases. In this study, we consider only two components for the sake of simplicity, and thus the free surface of irregular waves can be expressed as follows:

$$\eta = \frac{\eta_0}{2}\sin\left(k_1 x - \omega_1 t\right) + \frac{\eta_0}{2}\sin\left(k_2 x - \omega_2 t\right) \tag{31}$$

where k_1 and k_2 are the wavenumbers corresponding to ω_1 and ω_2. The values of ω are set as $\omega_1=\omega$ (1−0.1); $\omega_2=\omega(1+0.1)$. The wave amplitude, wave period and water depth are the same as in Figs. 2 and 3. The horizontal and vertical velocities satisfy the same relationship as shown in Eq. (27). Figure 4 shows the comparison between the numerical solutions and the analytical solution.

Figure 5 presents the errors induced by the numerical scheme. The general trends are almost the same as the regular wave cases. The numerical model predicts the free surface elevations well and the results produced using the Legendre interpolation and diagonal matrix show better predictions than those using Lagrangian interpolation. The averaged error of La-B is 2.85 times larger than that of Le-B and the maximum is almost ten times when the number of elements per wave length becomes two, as the regular case shows.

Finally, the solitary wave is modeled to examine the accuracy of the method. The solitary wave that propagates balancing the dispersion and the nonlinearity has been widely used for studies on wave nonlinearity. Wei and Kirby (1995) presented the following analytical solutions for Nwogu (1993)'s Boussinesq equations:

$$\xi\left(x,t\right) = a_1 \operatorname{sech}^2\left(b\left(x-ct\right)\right) + a_2 \operatorname{sech}^4\left(b\left(x-ct\right)\right) \tag{32}$$

$$u\left(x,t\right) = a\operatorname{sech}^2\left(b\left(x-ct\right)\right) \tag{33}$$

where $c=\sqrt{g(\eta_0+h)}$, and a_1, a_2, a, and b are defined as follows:

$$a_1 = \frac{C^2-gh}{3\left[\left(\alpha+1/3\right)gh-\alpha C^2\right]}h \tag{34a}$$

$$a_2 = \frac{\left(C^2-gh\right)^2}{2ghC^2}\frac{\left[\left(\alpha+1/3\right)gh+2\alpha C^2\right]}{\left[\left(\alpha+1/3\right)gh-\alpha C^2\right]}h \tag{34b}$$

$$a = \frac{C^2-gh}{C} \tag{34c}$$

$$b = \left\{\frac{C^2-gh}{4\left[\left(\alpha+1/3\right)gh^3-\alpha h^2C^2\right]}\right\}^{1/2} \tag{34d}$$

where $\alpha=\theta^2/2+1/2$. As in the modeling of the regular waves, the initial and boundary conditions of η, u, and w were set using Eqs. (32) and (33), and

the numerical simulations were conducted by changing the number of elements in the domain. The calculation conditions were water depth of 0.45 m, wave height of 0.045 m, and domain length of 100 m. The time interval was set as 0.01 sec to minimize any error related to the time difference.

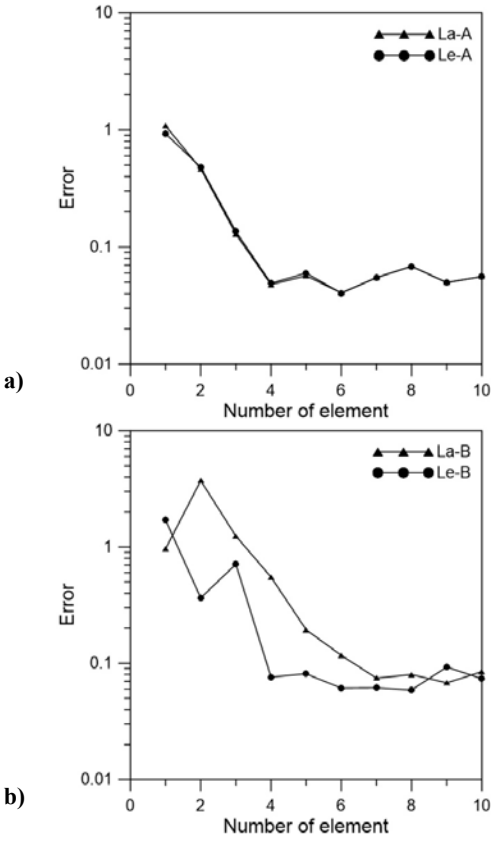

Fig. 5. Errors estimated by the Lagrangian (La) and Legendre (Le) interpolation functions for the irregular waves: a) full matrix; b) diagonal matrix.

In Fig. 6, the wave elevations at t = 5 and 30 sec from the simulations with 100 elements are presented. When the section was sufficiently divided, the numerical solutions of both the Lagrangian and Legendre interpolation functions agree well with the analytical solutions, as shown in the figure.

Figure 7 compares the error defined by Eq. (31) between the numerical solutions and the analytical solutions of the solitary wave. When analytically integrating the full mass matrix of Eq. (14), the errors of the Lagrangian (La-A) and Legendre interpolation functions (Le-A) are similar. As the number of elements increases within the calculation domain, the error tends to decrease. With 90 elements or more, the error appears to begin to converge to O (10^{-2}). Unlike the full matrix calculation, there is a big difference in the diagonal matrix calculation between the mass lumping for the Lagrangian function (La-B) and the numerical integration (Le-B). When the number of elements is small, the error of Le-B is larger than Le-A, showing values almost 1.5 times larger. When the Legendre interpolation function (Le-B) is used, the error of the approach converges to O (10^{-2}) when there are 130 elements. Meanwhile, in the case of the Lagrangian interpolation function (La-B), the error does not appear to converge even until 250 elements. In terms of the error convergence, the diagonal matrix calculation is not relatively good.

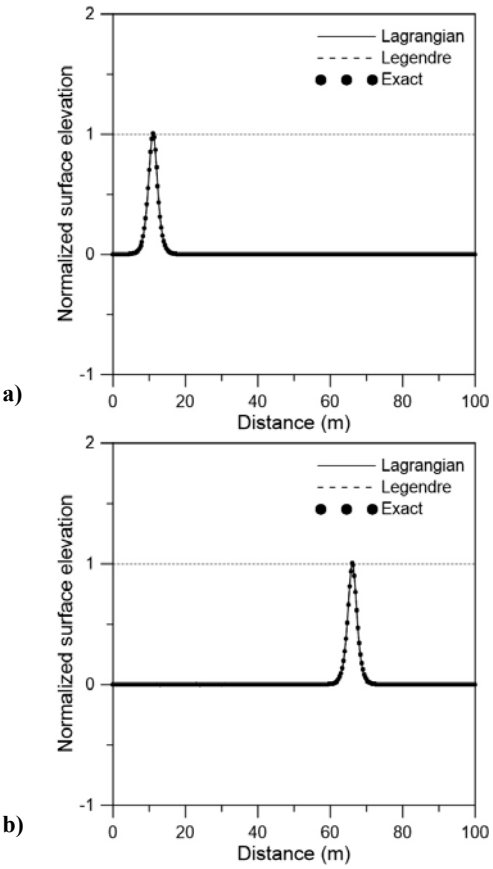

Fig. 6. Comparison of the solitary wave solutions with the analytical solution for: a) t = 5 sec; b) t = 30 sec.

In order to assess the efficiency of the methods, the calculation time until the acceptable accuracy shown in Figs. 3 and 7 is reached is examined through the FORTRAN function, cpu_time. Since the methods for the full matrix calculation (La-A, Le-A) have similar accuracy for all cases, one of those, La-A, was used as the representative case of the full matrix calculation. Thus, for the comparison of the calculation time, the method of full matrix calculation (La-A) and two methods of direct matrix calculation (La-B, Le-B) are examined for the regular and solitary waves in Fig. 8.

Assuming the acceptable accuracy as O (10^{-1}), the number of elements per wave length of the regular waves are 3, 6, and 4 for La-A, La–B, and Le-B, respectively. As for the solitary wave, 50, 100, and 50 elements for La-A, La–B, and Le-B, respectively, for the calculation domain of 100 m are used for the error convergence. The calculation time for the calculation domain with the fixed elements giving acceptable accuracy is compared in Fig. 8. Note that the calculation time

means the running time for one time interval (Δt). For both applications for the regular waves and the solitary wave, the diagonal matrix calculation with the Legendre interpolation function (Le-B) is conducted with the shortest time. The full matrix calculation (La-A) requires a much larger calculation time, which means the methods for the full matrix are too inefficient. As the spatial domain increases, i.e., the matrix size becomes larger, the calculation time increases exponentially, and consequently the difference among the methods also increases. In other words, as the size of the matrix increases, the method of Le-B becomes more efficient. For the regular waves, the running times for largest domain are 128.0, 44.37, 37.22 sec for La-A, La-B, Le-B, and 185.72, 65.30, 22.35 sec for the case of solitary wave, respectively. Note that the numerical values obtained in the calculation are not absolute ones. This implies that the comparison results may be changed depending on domain size or desired accuracy. However, the diagonal matrix calculation with the Legendre interpolation function (Le-B) is found to be efficient in overall finite element methods, especially for a large domain.

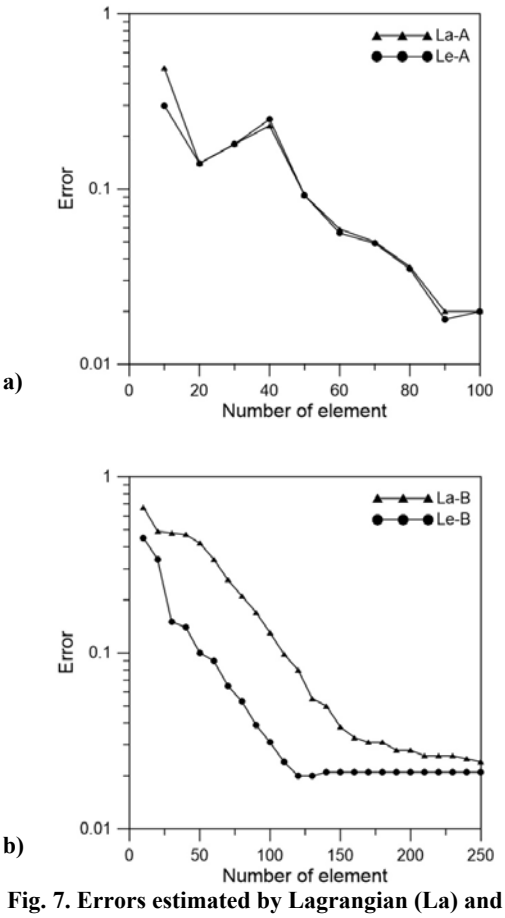

Fig. 7. Errors estimated by Lagrangian (La) and Legendre (Le) interpolation functions for the solitary wave: a) full matrix; b) diagonal matrix.

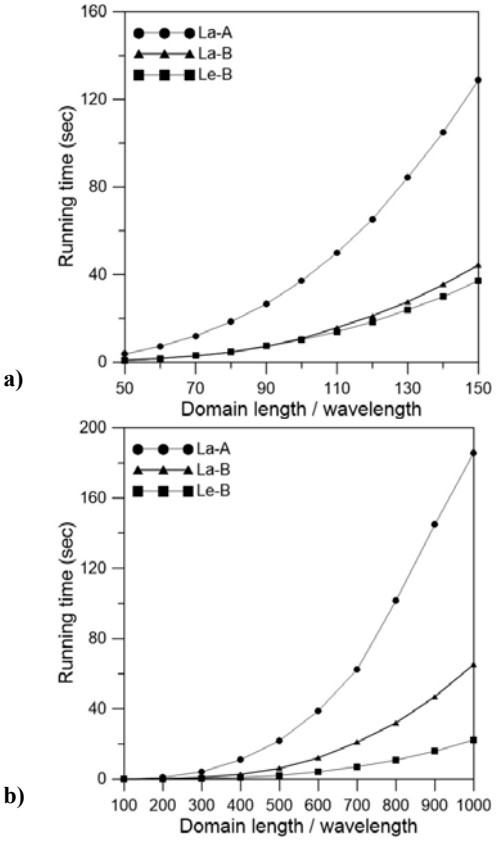

Fig. 8. Comparison of the running time obtained by the Lagrangian (La) and Legendre (Le) interpolation functions for: a) regular waves; b) solitary wave.

4. CONCLUSIONS

This study compared the applications of the Lagrangian and Legendre interpolation function with third-order to a finite element model for wave simulations. The existing study for the comparison (Eskilsson and Sherwin 2003) targets the higher-order Legendre cardinal interpolation function and the linear interpolation function, but lacks an explanation of whether the results by the Legendre function are acquired from its own characteristics or attributed to the higher-order interpolation function. This study investigated the features of the Legendre interpolation function with the interpolation functions of the same degree. For a higher-order finite element model, the Lagrangian higher-order polynomial is used to position nodes with the same interval. In this case, it takes a relatively long time because the size of a matrix becomes large while the mass lumping to solve such a problem reduces the accuracy of solutions in return. When the Legendre interpolation function is used, however, those problems can be lessened through numerical integration. In the application of the Legendre interpolation function for the FEM modeling of regular, irregular and solitary waves, the accuracy of the full matrix calculation is better than that of the diagonal matrix calculation. In the diagonal matrix calculation, the method that used the Legendre interpolation function (Le-B) is more accurate than the mass lumping for the Lagrangian

function. Although the solution accuracy of the full matrix calculation is better for a certain number of elements, the calculation time shows a different tendency. For the accuracy of O (10^{-1}), the full matrix calculation for the regular and irregular waves simulation takes much longer time than the diagonal matrix calculation. The Legendre interpolation function for the diagonal matrix calculation takes a shorter time than the mass lumping for the Lagrangian function as the domain becomes larger. In the modeling of the solitary wave, the diagonal matrix calculation with the Legendre interpolation function shows a big difference in the calculation time from the mass lumping for the Lagrangian function, and the difference gets larger with the increase of the domain. Consequently, when the full matrix for FEM is solved, the most accurate results can be obtained with a smaller number of elements if the calculation time does not need to be considered. If the calculation time is crucial or a large domain needs to be modeled, however, the application of the Legendre interpolation function to the diagonal matrix for FEM can obtain the desired accuracy to some degree while reducing the calculation time.

ACKNOWLEDGEMENTS

This study is supported partially by the Basic Research Program (NRF-2012R1A1A1011884) of the National Research Foundation of Korea, funded by the Ministry of Education, Science and Technology and partially by Korea Institute of Civil Engineering and Building Technology (KICT Project No. 2016-0142).

REFERENCES

Adytia, D. and E. van Groesen (2012). Optimized variation 1D Boussinesq modelling of coastal waves propagating over a slope. *Coastal Engineering 64*, 139-150.

Eskilsson, C. and S. J. Sherwin (2003). An hp/spectral element model for efficient long-time integration of Boussinesq-type equations. *Coastal Engineering Journal 45*(2), 295-320.

Eskilsson, C., S. J. Sherwin, and L. Bergdahl (2006). An unstructured spectral/hp element model for enhanced Boussinesq type equations. *Coastal Engineering 53*, 947-963.

Gobbi, M. F. and J. T. Kirby (1999). Wave evolution over submerged sills: tests of a high-order Boussinesq model. *Coastal Engineering 37*, 57-96.

Karniadakis, G. E. and S. J. Sherwin (2005). *Spectral/hp Element Methods for CFD.* Oxford, UK: Oxford University Press.

Kato, S., T. Takagi and M. Kawahara (1998). A finite element analysis of mach reflection by using the Boussinesq equation. *International Journal of Numerical Methods in Fluids 28*, 617-631.

Kim, G., C. Lee and K. Suh (2009). Extended Boussinesq equations for rapidly varying topography. *Ocean Engineering 36*, 842-851.

Madsen, P. A., I. R. Murray and O. R. Sorensen (1991). A new form of the Boussinesq equations with improved linear dispersion characteristics. *Coastal Engineering 15*(4), 371-388.

Nwogu, O. (1993). Alternative form of Boussinesq equations for nearshore wave propagation. *Journal of Waterway Port Costal and Ocean Engineering 119*, 618-638.

Panchang, V., W. Chen, B. Xu, K. Schlenker, Z. Demirbilek and M. Okihiro (2000). Exterior bathymetric effects in elliptic harbor wave models. *Journal of Waterway Port Costal and Ocean Engineering 126*, 71-78.

Park, W. S., I. S. Chun and W. M. Jeoung (1994). Infinite element for the analysis of harbor resonances. *Journal of Korean Society of Coastal and Ocean Engineers 6*, 139-149.

Patera, A. T. (1984). A spectral element method for fluid dynamics: Laminar flow in a channel expansion. *Journal of Computational Physics 54*, 468-488.

Peregrine, D. H. (1967). Long waves on a beach. *Journal of Fluid Mechanics 27*, 815-827.

Roeber, V., K. F. Cheung and M. H. Kobayashi (2010). Shock-capturing Boussinesq-type model for nearshore wave processes. *Coastal Engineering 57*, 407-423.

Sanz-Serna, J. M. and I. Christie (1981). Petrov-Galerkin methods for nonlinear dispersive waves. *Journal of Computational Physics 39*, 94-102.

Walkley, M. and M. Berzins (1999). A finite element method for the one-dimensional extended Boussinesq equations. *International Journal of Numerical Methods in Fluids 29*, 143-157.

Walkley, M. and M. Berzins (2002). A finite element method for two-dimensional extended Boussinesq equation. *International Journal of Numerical Methods in Fluids 39*, 865-885.

Wei, G. and J. T. Kirby (1995). A time-dependent numerical code for extended Boussinesq equations. *Journal of Waterway Port, Coastal and Ocean Engineering 121*, 251-261.

Wei, Z. and Y. Jia (2014a). Simulation of nearshore wave processes by a depth-integrated non-hydrostatic finite element model. *Coastal Engineering 83*, 93-107.

Wei, Z. and Y. Jia (2014b). Non-hydrostatic finite element model for coastal wave processes. *Coastal Engineering 92*, 31-47.

Witting, J. M. (1984). A unified model for the evolution of nonlinear water waves. *Journal of Computational Physics 56*(2), 203-239.

Woo, S. B. and P. L. F. Liu (2001). A Petrov-Galerkin finite element model for one-dimensional fully non-linear and weakly dispersive wave propagation. *International Journal of Numerical Methods in Fluids 37*, 541-575.

Woo, S. B. and P. L. F. Liu (2004a). Finite-element model for modified Boussinesq equations. I: Model development. *Journal of Waterway Port Costal and Ocean Engineering 130*, 1-16.

Woo, S. B. and P. L. F. Liu (2004b). Finite-element model for modified Boussinesq equations. II: Applications to nonlinear harbor oscillations. *Journal of Waterway Port Costal and Ocean Engineering 130*, 17-28.

Zienkiewicz, O. C. and R. L. Taylor (1989). *The Finite Element Method Vol. 1: Basic Formulation and Linear Problems*, McGraw-Hill, Maidenhead, England.